Biochimica et Biophysica Acta 939 (1988) 89–101
Elsevier

BBA 73948

Influenza virus–model membrane interaction. A morphological approach using modern cryotechniques

Koert N.J. Burger [a], Gerhard Knoll * and Arie J. Verkleij [b]

[a] *Institute of Molecular Biology and Medical Biotechnology, and* [b] *Department of Molecular Cell Biology, University of Utrecht, Utrecht (The Netherlands)*

(Received 2 November 1987)

Key words: Influenza B virus; Membrane fusion; Fast freezing; Freeze-fracture; Freeze-substitution; Thin sectioning; Electron microscopy

The membrane fusion activity of influenza virus was characterized morphologically using a model system composed of a highly purified influenza B virus suspension and ganglioside-containing zwitterionic liposomes. Electron microscopical analysis was performed after a combination of fast-freezing with either freeze-fracture or freeze-substitution–thin sectioning, ensuring maximal time resolution and avoiding preparation artifacts. In a parallel fluorescence 'lipid mixing' fusion assay, influenza virus-membrane fusion was characterized biochemically. Biochemical and morphological data are in full agreement, indicating negligible membrane fusion activity at neutral pH and high fusion activity at low pH. The freeze-fracture morphology strongly suggests a local point contact between viral and liposomal membrane at neutral pH, and a local point fusion mechanism for influenza virus-membrane fusion upon lowering of the pH. Fusion is followed by lipid mixing, lateral diffusion of viral spike proteins and exposure of viral contents at the inner liposomal surface.

Introduction

One of the best characterized protein-modulated membrane fusion events is the fusion of enveloped animal viruses with their target membranes [1]. Among these enveloped animal viruses, influenza virus has been studied most extensively. Influenza virus enters the cell by receptor-mediated endocytosis [2]. As a result of gradual acidification of the endosomal compartment (by an ATP-dependent proton pump [3]), the viral membrane fuses with the endosomal membrane and the viral nucleocapsid is released into the cytoplasm.

This low-pH activated fusion process is mediated by the viral hemagglutinin glycoprotein (HA [4,5]), which together with a second spike protein, the neuraminidase, constitutes the outer shell of the influenza virion [6]. The influenza hemagglutinin is involved in both initial attachment of the virus to sialic acid containing receptors on the target membrane [7] and in the fusion process itself [8,9]. The three-dimensional structure of the trimeric ectodomain of the hemagglutinin glycoprotein has been determined from X-ray studies at 3 Å resolution [10]. The fusion activity is thought to reside in the extremely hydrophobic and highly conserved N-terminal part of subunit 2 of the hemagglutinin glycoprotein, which is exposed after

* Present address: Fakultät für Biologie, Universität Konstanz, Postfach 5560, D-7750 Konstanz, F.R.G.

Abbreviations: FFFS, fast-freeze freeze-substitution; RET, resonance energy transfer; buffer A, 50 mM Tris-HCl, 100 mM NaCl (pH 7.4).

Correspondence: K.N.J. Burger, Institute of Molecular Biology and Medical Biotechnology, University of Utrecht, Padualaan 8, 3584 CH Utrecht, The Netherlands.

an irreversible conformational change of the hemagglutinin molecule at low pH [11,12]. This N-terminal fusion sequence is generally thought to interact with the target membrane, forcing viral and target membrane together and inducing them to fuse by some still unknown mechanism [12–14].

Despite the efforts made in numerous biochemical and biophysical studies (for review, see Ref. 1) many questions, especially with regard to the mechanism and the intermediates of the actual joining of the two lipid bilayers, have remained unsolved. Some of these questions could possibly be solved by using an ultrastructural approach.

The principal aim of the work presented here was a morphological characterization of the membrane fusion activity of influenza virus.

Since membrane fusion has proven to be an extremely rapid event [15], controlled induction of fusion by lowering of the pH was combined with synchronized fast-freezing, in order to try and catch early fusion intermediates, and follow the fate of viral intramembrane proteins after the final mergence of viral and liposomal membrane. Analysis was performed using freeze-fracture electron microscopy, and complemented by a freeze-substitution low-temperature embedding technique [16] (i.e. fast-freeze freeze-substitution–, or FFFS–, thin sectioning) avoiding artifacts caused by the chemical pretreatments during classical chemical fixation, cryoprotection and dehydration procedures [17]. FFFS–thin sectioning avoids extraction of phospholipids [18] and has proven to be a reliable complement to freeze-fracturing, even in the analysis of pure lipid systems [19]. In a parallel fluorescence 'lipid mixing' fusion assay influenza virus-liposome fusion was characterized biochemically.

Evidence will be presented in favour of a local point fusion mechanism for influenza virus-membrane fusion. Membrane fusion is followed by mixing of viral and liposomal lipids and by diffusion of viral spike proteins into the liposomal membrane.

Materials and Methods

Materials

Egg phosphatidylcholine (egg PC), egg phosphatidylethanolamine (egg PE) and cholesterol were purchased from Sigma Chemical Co. (St. Louis, MO). The disialoganglioside IV^{3}NeuAc,-II^{3}NeuAc-GgOse$_4$Cer (G_{D1a}) was obtained from Supelco, Inc. (Bellefonte, PA). *N*-(lissamine rhodamine B sulfonyl)phosphatidylethanolamine (N-Rh-PE) and *N*-(7-nitrobenz-2-oxa-1,3-diazol-4-yl)phosphatidylethanolamine (N-NBD-PE) were from Avanti Polar Lipids Inc. (Birmingham, AL). *n*-Octyl-β-D-glucopyranoside (*n*-octyl glucoside) was obtained from Calbiochem-Behring Corp. (La Jolla, CA). The neuraminidase inhibitor 2-deoxy-2,3-dehydro-*N*-acetylneuraminic acid was purchased from Boehringer Mannheim Biochemicals (Mannheim, F.R.G.). Glycerol (anhydrous, p.a.) and potassium tartrate were obtained from Fluka AG (Buchs, CH) and Baker Chemical Co. (Phillipsburg, NJ), respectively. All other reagents and chemicals were of analytical grade.

Virus

Egg-grown influenza B/USSR/6/80 virus was a kind gift from J. Jacobs, Duphar B.V. (Weesp, The Netherlands). The virus had been inactivated by β-propiolacton and had been purified by three successive (large scale) sucrose gradient centrifugation steps. The virus was stored under sterile conditions at 4°C.

In the final purification, the virus was first pelleted onto a cushion of 50% glycerol in buffer A (50 mM Tris-HCl, 100 mM NaCl (pH 7.4)) by centrifugation at 110000 × *g* for 60 min, 4°C and resuspended overnight in a small volume of buffer A. Subsequently, the virus was isopycnically banded on 5–50% potassium tartrate gradients (w/v in buffer A) using a SW41 Beckman rotor (100000 × *g*, overnight, 4°C). The high density band was collected and the virus pelleted and resuspended in buffer A as above. The protein concentration was determined under the addition of Triton X-100 at a final concentration of 0.5%, using a protein determination set from Pierce Chem. Co. (Rockford, IL). The phospholipid to protein ratio of the virus was taken to be 175 nmol of phospholipid phosphorus/mg of protein [20]. The virus suspension was stored at 4°C and was used within 5 days after the final purification.

Liposomes

Large unilamellar vesicles (egg PE/egg

PC/cholesterol, 1 : 1 : 2 molar ratio) containing 5 mol% (of total lipid) of the ganglioside G_{D1a} and 1 mol% each of two fluorescent probes, N-NBD-PE and N-Rh-PE, were prepared by *n*-octyl glucoside dialysis according to Van Meer et al. [21], or alternatively by extrusion of freeze-thawed multilamellar vesicles through two stacked polycarbonate filters (pore size 400 nm) as described by Mayer et al. [22] using the extruder manufactured by Lipex Biomembranes Inc. (Vancouver, Canada). The vesicles, suspended in buffer A, had an approximate mean diameter, depending on the method of preparation, of 185 nm and 155 nm, respectively. Whereas the percentage of vesicles with a unilamellar appearance was calculated to be more than 90% and more than 80%, respectively (both parameters based on thin-section micrographs). The phospholipid phosphorus concentration was determined by the method of Böttcher et al. [23].

Fluorescence fusion assay

Virus-liposome fusion was characterized biochemically using a fluorescence fusion assay according to Struck et al. [24]. Fusion results in the mixing of viral and liposomal lipids and a concomitant decrease in the efficiency of energy transfer between the two fluorescent probes originally incorporated in the liposomes (N-NBD-PE, N-Rh-PE, 1 mol% each).

Measurements were carried out in a final volume of 1.4 ml in a glass cuvette, at a liposome phospholipid phosphorus concentration of 5 μM. A small volume (15 μl) of purified influenza virus suspension (2.6 mg viral protein per ml) was injected using a Hamilton syringe. The increase of N-NBD-PE fluorescence was recorded continuously using a Perkin-Elmer MPF-3 fluorimeter and excitation and emission wavelengths of 465 nm and 530 nm, respectively. All measurements were carried out under continuous stirring at 37 °C, unless stated otherwise.

The fluorescence scale was calibrated by taking the initial N-NBD-PE fluorescence intensity, when no lipid mixing has yet occurred, as 0%, and the N-NBD-PE fluorescence intensity at infinite probe dilution as 100%. The 100% value was determined by addition of Triton X-100 (0.1% v/v). The fluorescence scale was not corrected for the effect of Triton X-100 on the quantum yield of N-NBD-PE.

During the actual measurements, influenza virus and liposomes, prepared by *n*-octyl glucoside dialysis, were incubated for 10 min at pH 7.4 (buffer A), after which the pH was adjusted to pH 5.5 by injecting 60 μl of a 100 mM succinic acid, 100 mM NaCl solution. Identical results were obtained by first adjusting the pH and then adding the virus.

The pH profile of influenza virus-liposome fusion was determined by adjusting the pH of buffer A by adding the appropriate amount of 100 mM succinic acid, 100 mM NaCl solution or, with identical results, by using a 10 mM Pipes, 5 mM Hepes, 15 mM sodium citrate, 135 mM NaCl buffer adjusted to the desired pH.

The presence of a neuraminidase inhibitor (10 mM 2-deoxy-2,3-dehydro-*N*-acetylneuraminic acid) did not influence the fluorescence measurements.

Electron microscopy

Virus and liposomes were mixed to yield a viral to liposomal phospholipid phosphorus molar ratio of approximately 1 to 2. Comparable results were obtained with liposomes prepared by either *n*-octyl glucoside dialysis or the extrusion procedure. Neuraminidase inhibitor was added to a final concentration of 10 mM. Typically 30 μl influenza virus suspension (13.2 mg viral protein per ml), 20 μl liposomes (phospholipid phosphorus concentration 7.2 mM) and 16 μl neuraminidase inhibitor (12 mg/ml) were added together and incubated at pH 7.4 (buffer A) for 30 min on ice. Small aliquots (2 μl) were mixed 1 to 1 (v/v) with a low-pH buffer (50 mM succinic acid-NaOH, 100 mM NaCl (pH 5.2)) to give a final pH 5.4. Samples (1 μl) were taken before and after the pH drop. Low-pH incubation time and temperature were varied (5 s to 30 min, 20 °C or 37 °C).

The samples were transferred to a sandwich composed of a plastic disc, a spacer and a copper cover, as described by Knoll et al. [25]. The sandwich samples were fast-frozen by plunging them into liquid propane (−190 °C), using a plunge freezing device (KF80) manufactured by Reichert Jung (Wien, Austria). No cryoprotectants were used. The sandwiches were stored in liquid nitrogen and used both for freeze-fracture as well

as freeze-substitution and low-temperature plastic embedding (FFFS–thin sectioning).

For freeze-fracture the sandwiches were transferred to a Balzers BAF 300 freeze-etch machine, fractured and replicated following established procedures. The replicas were stripped off and cleaned with dilute chromic acid and distilled water according to Costello et al. [26].

Freeze-substitution and low-temperature plastic embedding were performed essentially according to Müller et al. [27] and Humbel et al. [16], using an Auto CS unit (Reichert Jung, Wien, Austria). The sandwiches were fractured under liquid nitrogen to remove the copper cover. The plastic discs together with the spacer and adhering parts of the sample were transferred to the substitution medium consisting of 1% OsO_4, 0.5% UO_2Ac and 3% glutaraldehyde in MeOH. After a period of 10 h at $-80\,^{\circ}C$ the temperature was slowly raised to $-45\,^{\circ}C$ (4 C°/h), the specimens were washed with methanol, gradually infiltrated with the hydrophobic Lowicryl HM20 resin, and finally polymerized by ultraviolet light at $-45\,^{\circ}C$ for 24 h. The temperature was raised to room temperature and the specimens were further hardened under ultraviolet light illumination for at least 24 h. Thin sectioning was performed according to standard procedures. Ultrathin sections were stained for 10 min with 2% potassium manganate in distilled water.

Freeze-fracture replicas and ultrathin Lowicryl sections were examined with a Philips EM 420 at 80 kV.

Results

Purity of the virus suspension

Freeze-fracture allows for a critical evaluation of the purity of the virus suspension (Fig. 1). Even after a (large scale) purification involving three subsequent sucrose gradient centrifugation steps, impurities in the virus suspension are obvious (Fig. 1a). The freeze-fracture morphology of these impurities, most likely pieces of infected chorioallantoic membrane, is such that in the final virus-liposome mixtures these structures could easily be misinterpreted as being intermediates of a virus-membrane binding and fusion sequence.

Further purification of the virus suspension involved an additional potassium tartrate gradient centrifugation step, and a virus suspension was obtained which, as judged from freeze-fracture electron micrographs (Fig. 1b), showed a very high degree of purity.

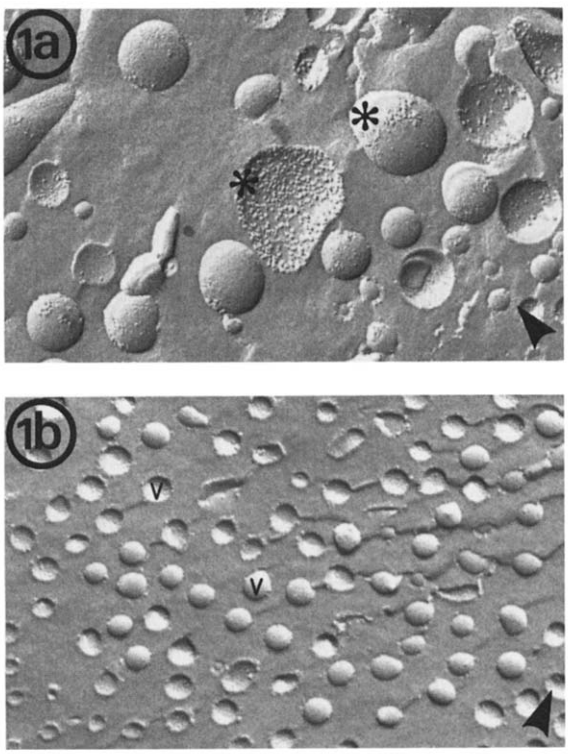

Fig. 1. Freeze-fracture electron micrograph of the influenza B virus suspension before (a) and after (b) the final purification. Impurities (*) in (a) are removed by a potassium tartrate gradient centrifugation step, yielding a pure virus suspension (b) with virions (V), fairly uniform in shape and approx. 90 nm in diameter (size of the naked virion i.e. without the spike proteins). Final magnification 43000×.

Biochemical characterization of influenza virus–liposome interaction

Fusion of influenza B virus with liposomes containing the virus receptor-ganglioside G_{D1a} was measured using a fluorescence fusion assay according to Struck et al. [24]. Using this method the kinetics and final extent of viral and liposomal lipid mixing can be determined.

Fig. 2 shows the pH dependence and time-course of virus-membrane fusion. At neutral pH the initial rate (Fig. 2) and the final extent (data

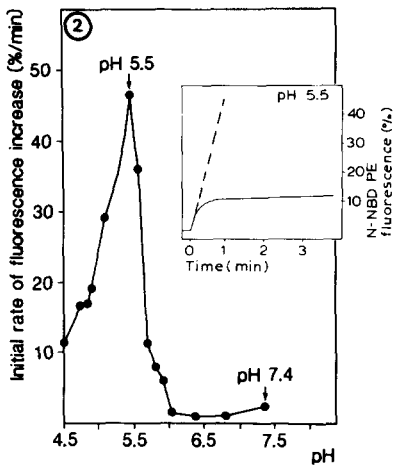

Fig. 2. Initial rate of influenza virus-liposome fusion as a function of pH. Rates of N-NBD-PE fluorescence increase were calculated, for different pH values, from the tangents drawn to the steepest parts of the fusion curves (e.g. — — — inset). The inset shows the time-course of N-NBD-PE fluorescence increase (———) at the pH optimum for virus-membrane fusion (pH 5.5). All measurements were carried out as described under Material and Methods at 37 °C.

not shown) of fusion are both very low. Upon lowering the pH a fast fusion event is initiated, the rate of which is strongly pH (Fig. 2) and temperature dependent (data not shown).

The steep pH-dependence of virus-membrane fusion, its high initial rate at the pH optimum (pH 5.5, Fig. 2), together with the high purity of the influenza B virus suspension based on freeze-fracture electron microscopy, justify the use of this particular influenza virus suspension in the morphological characterization of influenza virus-membrane fusion.

Morphological characterization of influenza virus–liposome interaction at neutral pH: binding

Fig. 3 shows freeze-fracture and FFFS–thin-section morphology of influenza virus-liposome mixtures, fast-frozen and processed after 30 min incubation at pH 7.4, 0 °C, in the presence of a neuraminidase inhibitor. The neuraminidase inhibitor was added in order to prevent any action of the viral neuraminidase and subsequent release of originally liposome-bound virus as a consequence of ganglioside breakdown [28]. The addition of a neuraminidase inhibitor did not influence the fusion characteristics as measured with the fluorescence fusion assay (data not shown).

Binding of influenza virus to receptor-ganglioside-containing liposomes at neutral pH leads to pronounced local membrane deformations, visible on both convex and concave fracture faces of the liposomal membrane (Figs. 3a and 3b, respectively). Based on morphological criteria these deformations of the liposomal membrane can be subdivided into two groups.

Protrusions of the convex liposomal fracture face, 35 to 60 nm in diameter, and complementary invaginations of the concave fracture face predominate (● in Figs. 3a and 3b, respectively). These protrusions of the convex liposomal fracture face often bear two or more ill-defined particles (→ in Fig. 3c), whereas occasionally one central and reasonably well-defined particle of 9 to 14 nm in size is observed (detail, Fig. 3c). The lack of ultrastructural detail does not allow for the determination of complementary pits, or particles, on the concave fracture face of the liposomal membrane.

Since the fluorescence fusion assay did not show any significant lipid mixing between viral and liposomal membranes at neutral pH, semifusion seems very unlikely at this stage. Therefore we propose that the central particle originates from a local point contact between the viral and liposomal membrane (see also Discussion). The protrusions bearing multiple ill-defined particles (→ in Fig. 3c) possibly represent early stages in virus-liposome adhesion.

Apart from protrusions of the convex fracture face, occasionally ringlike depressions on the convex fracture face and complementary protrusions of the concave fracture face are observed (△ in Figs. 3a and 3b, respectively).

These ringlike depressions on the convex fracture face might well represent early stages in an alternative virus-liposome binding process. A process in which through the interaction between viral spike proteins and liposomal receptor-gangliosides, a virion binds to a liposome, is partially engulfed and possibly 'endocytosed' by the liposome [29]. The possibility of a partial uptake of a virion in a endocytic-like event is further supported by the presence of an occasional, mem-

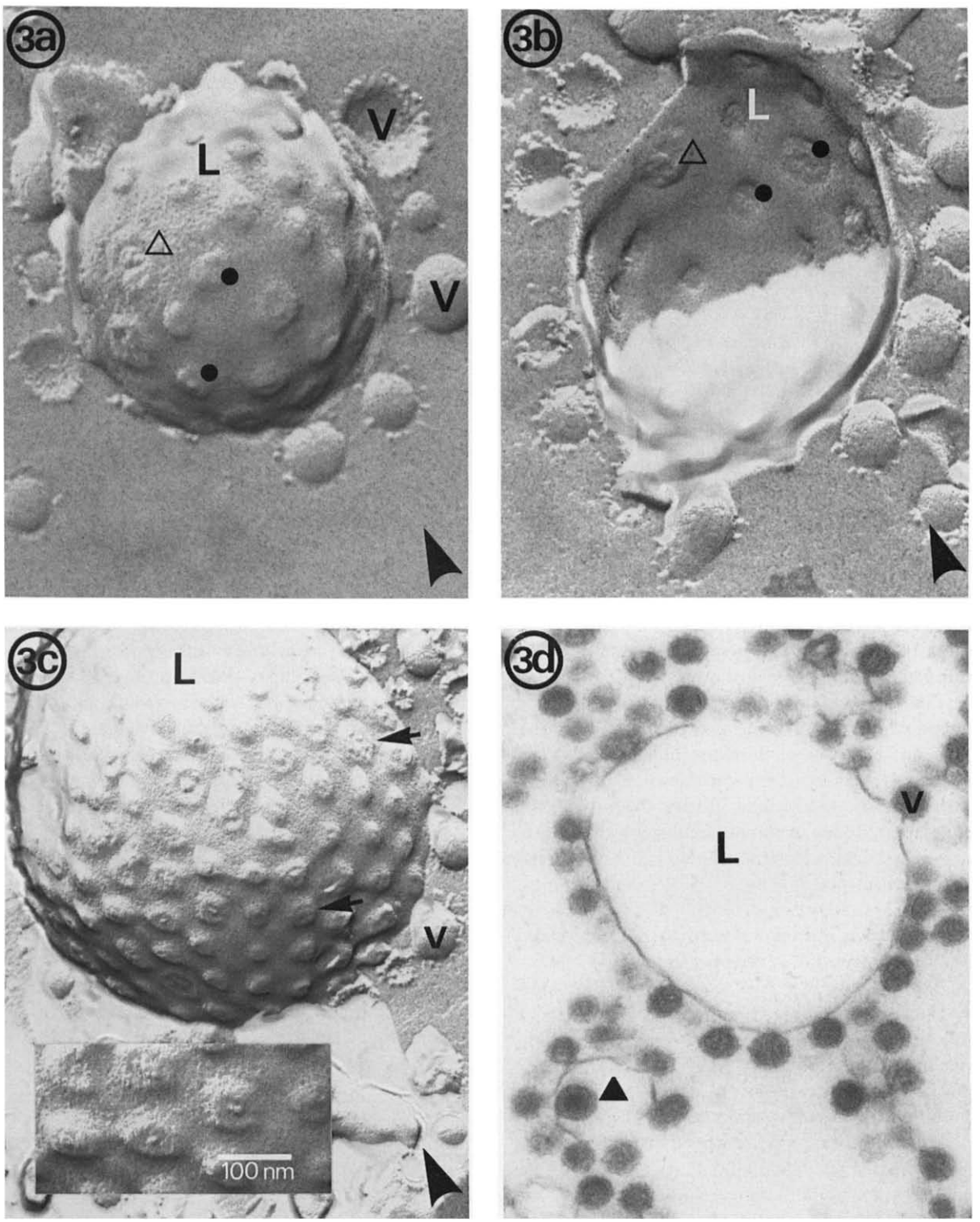
3a
L
V
V
3b
L
3c
L
v
100 nm
3d
L
v

brane surrounded, virion inside a liposome (most likely as the result of a fortunate cross-section through an almost entirely engulfed virion, ▲ in Fig. 3d). However, even under non-saturated conditions, i.e. a liposome with only a few virions bound (data not shown), partial engulfment of virions is relatively rare as compared with the more superficial binding and the local point contact between virus and liposomes described earlier.

The morphological data on influenza virus–liposome interaction at neutral pH are in full agreement with the results of the fluorescence fusion assay, demonstrating negligible influenza virus-membrane fusion at neutral pH. Membrane continuity between viral and liposomal membrane is not observed and, apart from an occasional particle present in the center of a deformation of the convex fracture face, both fracture faces of the liposomal membrane remain smooth, in sharp contrast to the situation after a pH drop.

Morphological characterization of influenza virus–liposome interaction at low pH: fusion

After binding of influenza virus to ganglioside-containing liposomes at neutral pH (30 min, 0 °C), samples were incubated at low pH and subsequently fast-frozen and processed for electron microscopy.

Low-pH incubation time and temperature were varied (5 s to 30 min, 20 °C and 37 °C). In initial attempts samples were frozen under early fusion conditions (5 s to 1 min after lowering the pH) in order to try and catch early fusion intermediates, i.e. intermediates of the actual joining of the viral and liposomal bilayer. These attempts were hampered by the heterogeneity of the fusion products (see Discussion); irrespective of low-pH incubation time and temperature, samples seemed to contain a variety of binding and fusion stages (data not shown).

In order to try and find clear-cut morphological evidence to prove that influenza virus-liposome fusion had in fact occurred, we examined samples incubated at low pH for longer time periods. Figs. 4 and 5 show freeze-fracture and FFFS–thin-section morphology of influenza virus-liposome mixtures incubated for approximately 2 min at pH 5.4 and 37 °C.

In the final analysis of these electron micrographs it is important to realize that relatively few virions, bound to liposomes at neutral pH, will actually fuse with these liposomes at low pH. This low fusion efficiency also accounts for the relatively low final extent of fusion observed in the fluorescence fusion assay (Fig. 2).

In spite of the low fusion efficiency influenza virus-membrane fusion can be demonstrated unequivocally in Figs. 4a–e and 5, as judged from three morphological criteria.

(1) Membrane continuity between viral and liposomal membrane, clearly seen in freeze-fracture electron micrographs (1 → in Fig. 4a). Membrane continuity is accompanied by aqueous channel formation, as observed in Figs. 4d and 4e (→). Occasionally a virion is seen to fuse with two liposomes at the same time (○ in Fig. 5).

(2) Diffusion of viral intramembrane particles into the liposomal membrane. After fusion intramembrane particles (IMPs) are present on the concave fracture face of the liposomal membrane. These IMPs and the IMPs present on the concave fracture face of the viral membrane share the same morphology and are interpreted as being representative of one or both viral spike proteins (2 → in Figs. 4a and 4b; see also Discussion). The integration of an influenza virion in the liposomal membrane and the subsequent lateral diffusion of viral spike proteins as a consequence of virus-membrane fusion, is beautifully demonstrated in Fig. 4c: a virion (V) is 'caught' just at the moment it flattens out into the liposomal surface and just before lateral diffusion of viral spike proteins takes

Fig. 3. Freeze-fracture and FFFS–thin-section morphology of influenza virus-liposome interaction at neutral pH (a–c, and d, respectively). Binding of influenza virus (V) to liposomes (L) for 30 min at 0 °C leads to pronounced local membrane deformations visible on convex and concave fracture faces of the liposomal membrane (a and b, respectively). Apart from ring-like deformations (△ in a and b), protrusions of the convex fracture face and complementary invaginations of the concave fracture face are present (● in a and b, respectively). The protrusions of the convex fracture face often bear multiple ill-defined particles (→ in 3c), and occasionally a single quite well-defined central particle is observed (c, detail). In a thin-section micrograph virions are occasionally seen inside a liposome (▲ in d). For details see text. Magnifications: (a and b) 136000×; (c and d) 77600×; inset (c) 136000×.

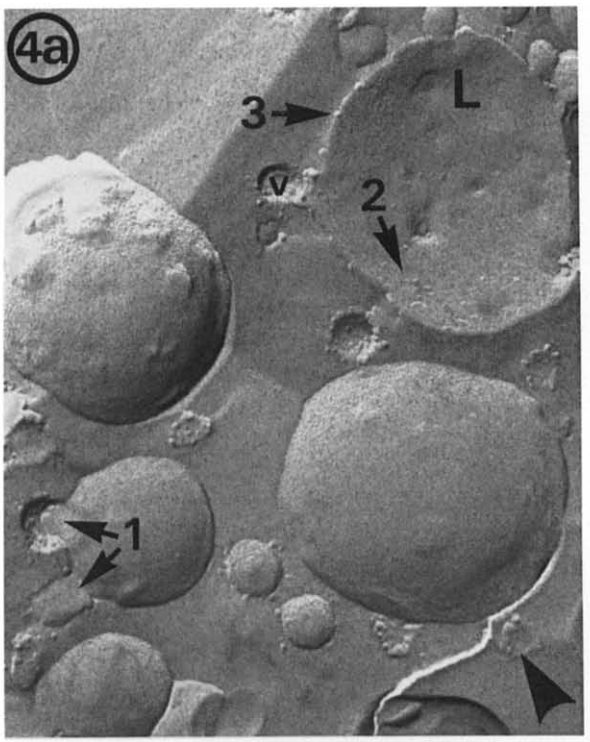
4a
L
3
v
2
1

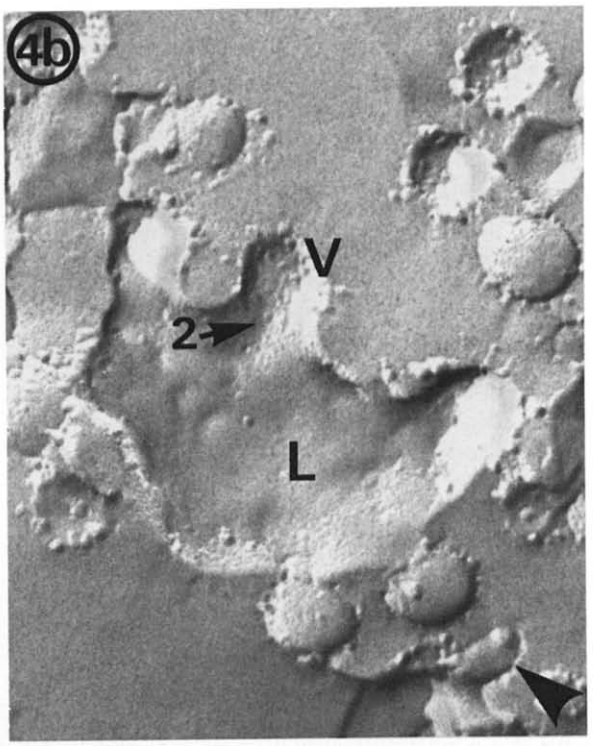
4b
V
2
L

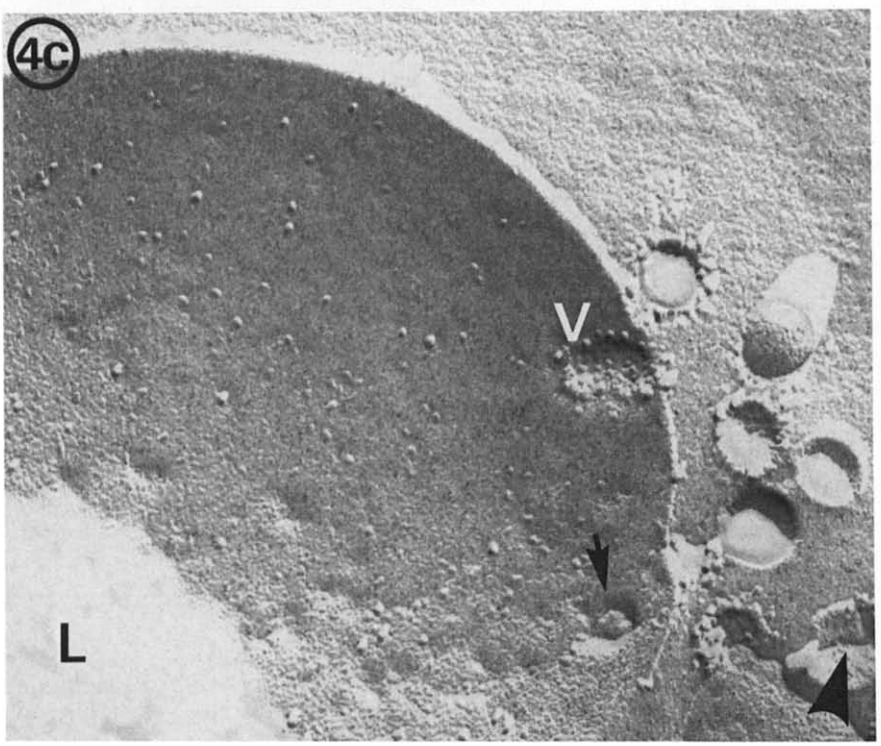
4c
V
L

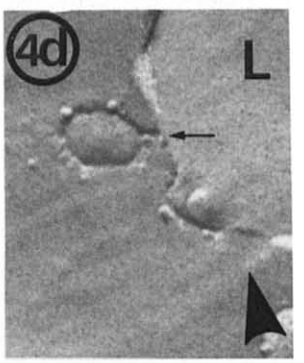
4d
L

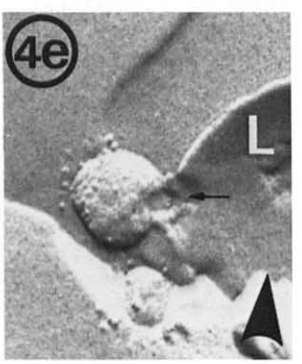
4e
L

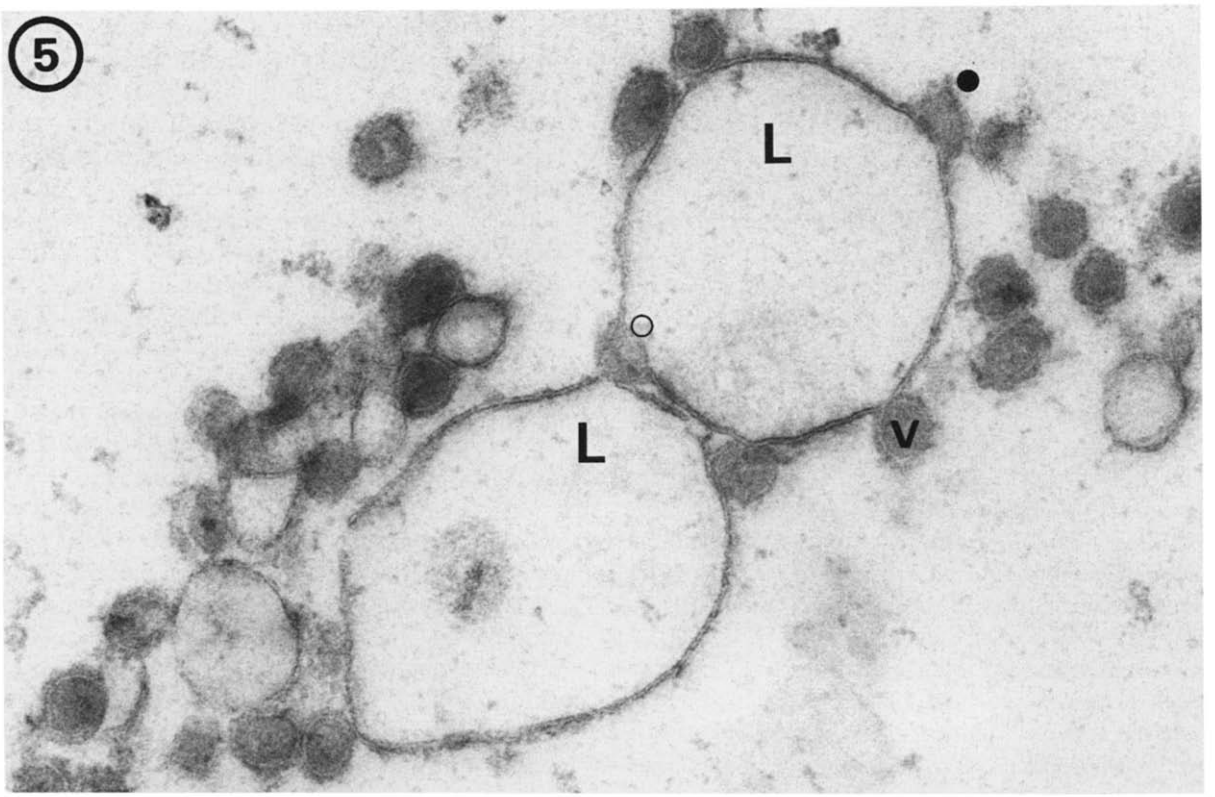

Fig. 5. FFFS–thin-section morphology of influenza virus–liposome interaction at low pH. Fused virions are observed (● and ○). The electron dense content of a fused virion is present at the liposomal inner surface (○). Magnification: 120000×.

place. The concave fracture face of the liposome is covered with IMPs, which most likely originated from earlier fused virions.

Additional proof for the diffusion of viral spike proteins into the liposomal membrane can be deduced from the presence of viral spikes in the fractured ice-matrix surrounding the liposomes (3 → in Fig. 4a).

(3) Presence of viral contents at the liposomal inner surface. In thin-section electron micrographs an influenza virion appears as an electron dense core surrounded by a membrane with a trilamellar appearance (Figs. 3d and 5). After virus-membrane fusion the electron dense core with the ribonucleoprotein as its main constituent is present at the inner liposomal surface (○ in Fig. 5).

Discussion

The techniques of freeze-fracture and FFFS–thin sectioning form a solid basis for the morphological characterization of membrane fusion

The membrane fusion activity of viruses has been subject of numerous biochemical and biophysical studies (for review, see Ref. 1), but up to now only a few thorough morphological studies of

Fig. 4. Freeze-fracture morphology of influenza virus–liposome interaction at low pH. Influenza virus-liposome fusion is demonstrated by membrane continuity (1 → in 4a), lateral diffusion of viral intramembrane particles (2 → in a and b), the presence of viral spikes in the fractured ice matrix surrounding the liposomes (3 → in a), and aqueous channel formation (→ in c). In (d, e) some details of freeze-fractured fused virions are shown, i.e. a cross-fractured and a partially cross-fractured virion, respectively. For details see text. Magnifications: (a) 97000×; (b) 150350×; (c–e) 126100×.

virus-membrane fusion have been published [2,29–34]. Most of these studies are based on classical thin-sectioning [2,30,31,34] or negative stain [29] electron microscopy and possibly suffer from preparation artifacts as a result of chemical fixation or dehydration. In extensive studies by Knutton [32,33] the fusion of human erythrocytes by Sendai virus is characterized mainly by freeze-fracture electron microscopy, omitting the dubious dehydration step. The results of these studies, again, have to be interpreted with caution since samples were chemically fixed and glycerol impregnated, and both treatments are known to cause changes in freeze-fracture morphology [35]. In this context it is important to realize that the frequent observation made in early freeze-fracture studies, namely intramembrane particle clearance from fusion-competent membrane areas [36,37], has been shown to be a preparation artifact [35,38,39].

Because its very high susceptibility to preparation artifacts and because membrane fusion has proven to be extremely fast (ms range [15,40,41]), only a combination of fast-freezing with a visualization technique, avoiding chemical pretreatments, should prove reliable [42].

In the present study fast-freezing, without any chemical pretreatment, is combined with freeze-fracture, and complemented by FFFS–thin sectioning. This thin-section technique almost entirely eliminates the main drawback of classical thin-section procedures, namely a nearly complete extraction of phospholipids during sample dehydration [18]. The potential use of FFFS–thin sectioning as a complementary technique to freeze-fracturing is demonstrated in Verkleij et al. [19], in which thin-section and freeze-fracture morphology of a pure lipid system were shown to be compatible.

We think that the combination of modern electron microscopical techniques has enabled one of the first reliable morphological characterizations of the biological membrane fusion activity of influenza virus to be made.

Fusion with ganglioside-containing zwitterionic liposomes closely reflects the biological fusion activity of influenza virus

The membrane fusion activity of influenza virus has been studied extensively using model systems in which biological or artificial membranes serve as fusion targets. Although Haywood and Boyer [43] reported neutral pH fusion of influenza virus with ganglioside-containing liposomes, most authors agree on the fact that biological fusion activity of influenza virus depends on a conformational change induced by low pH in the hemagglutinin glycoprotein [1]. By comparing the fusion activity of influenza virus towards erythrocyte ghost and artificial membranes [44] the conclusion seems justifiable that fusion of influenza virus with zwitterionic liposomes containing virus receptor-gangliosides, probably closely reflects the biological fusion activity of influenza virus.

In research concerning the fusion activity of influenza virus, influenza A strain viruses have been used almost exclusively. The amount of homology between type B and type A virus hemagglutinins is similar to the amount of homology observed among different type A virus hemagglutinins [45], and it seems very unlikely that the biological fusion activity of influenza A and B strain viruses should differ significantly.

In the present study, the interaction of an influenza B virus with ganglioside-containing liposomes was characterized.

The purity of the virus suspension is shown to be of crucial importance in the morphological characterization of influenza virus-liposome fusion, and was checked and confirmed by freeze-fracture electron microscopy (Fig. 1).

The fluorescence fusion assay (Fig. 2) shows a strongly pH-dependent mixing of viral and liposomal lipids. Lipid mixing, or fusion, at neutral pH is negligible.

Morphological characterization of the binding stage: local point adhesion precedes local point fusion

The absence of virus-membrane fusion at neutral pH is supported by the results of freeze-fracture and FFFS–thin-section electron microscopy.

At neutral pH, binding of influenza virus to ganglioside-containing liposomes leads to pronounced deformations of the liposomal membrane. The morphology of these deformations depends on the number of hemagglutinin spike proteins involved in the binding process.

A superficial binding of influenza virus pre-

dominates and gives rise to local protrusions of the convex liposomal fracture face, often bearing a central particle. The interpretation of this central particle is not straightforward and is complicated by the apparent absence of a complementary pit on the concave fracture face of the liposomal membrane (Fig. 3b). The size of the particles (9 to 14 nm in diameter) and the fact that they are quite well defined (inset, Fig. 3c) could lead to an interpretation as inverted micelles [46]. Inverted micelles are thought to occur at the joining stage of fusing membranes, a stage in which the outer lipid monolayers have joined but the inner have not (i.e. semifusion). Since semifusion of viral and liposomal membrane presupposes a partial mixing of their lipids, and no significant lipid mixing is observed with the fluorescence fusion assay at neutral pH, two possible explanations remain. If the central particles do represent a semifusion stage, dilution of the fluorescent probes (and possibly lipid mixing) either does not take place, or semifusion at neutral pH is very rare and therefore not detected with the fluorescence fusion assay.

Alternatively, the central particle could be interpreted as a prefusion structure. In the adhesion stage preceding membrane fusion and fission, local contact points or intermembrane attachment sites [46–48] could give rise to deflections in the freeze-fractured membranes because of local high curvature. Although the resultant cusp-like particles seen in pure lipid systems [46] are only similar and not identical to the particles described here, we favour this interpretation: a local point contact between viral and liposomal membrane is in agreement with both the irregular shape of the particles (Figs. 3a and 3c) and the negligible lipid mixing as monitored in the fluorescence fusion assay.

The involvement of progressively more hemagglutinin spike proteins in the binding process leads to partial engulfment of the virions by the liposome and results in the ringlike depressions visible on the convex liposomal fracture face (Fig. 3a). Based on negative stain electron microscopy, Haywood and Boyer [29] proposed a fusion mechanism for Sendai virus-liposome fusion, involving liposomal virus uptake and subsequent fusion of the viral membrane with the leading edge of the developing 'endocytic' vacuole. A similar mechanism was suggested for the fusion of influenza virus with ganglioside-containing liposomes at neutral pH [43]. Although, in our study, some evidence is presented in favour of an occasional partial engulfment of influenza virus by liposomes (Figs. 3a and 3d), fusion of viral and liposomal membrane at neutral pH was never observed.

Morphological characterization of the fusion process: local point fusion is followed by lipid mixing and the lateral diffusion of viral spike proteins

Because of the strict pH dependence of influenza virus-liposome fusion, binding of influenza virus to ganglioside-containing liposomes at neutral pH and induction of fusion by an instantaneous lowering of the pH, should provide the best possible synchronization and density of fusion events and maximize the chance of catching short-lived fusion intermediates. Nevertheless samples frozen under early fusion conditions (5 s to 1 min after lowering the pH) did not exhibit structural features which could be unequivocally identified as fusion intermediates. Even in the particularly well-synchronized system under study, fusion intermediates may have escaped detection because of their short lifetime [49] and resultant low density. In addition, the identification of possible fusion intermediates is further complicated by the heterogeneity of virus-liposome interactions observed at neutral pH, prior to the induction of fusion, and the probable 'non-ideal' synchronization of the fusion process.

Although early fusion intermediates could not be identified, the local point contact between viral and liposomal membrane seen at neutral pH strongly favours a local point fusion mechanism for influenza virus-membrane fusion. Interestingly, during budding of influenza virus from virus infected Madin-Darby canine kidney cells, a well-defined particle is observed, exactly at the connection between the joined viral and plasma membrane (Knoll et al., unpublished results). Both influenza virus-membrane fusion (and possibly virus-cell infection) and influenza virus budding seem to be governed by a local point fusion mechanism.

Fusion is followed by membrane continuity (Fig. 4a) and a concomitant mixing of viral and liposomal lipids (fluorescence fusion assay, Fig. 2),

and is accompanied by the formation of a connecting aqueous channel (Figs. 4d and 4e). The fused virion flattens out into the liposomal surface (Fig. 4c). Viral IMPs diffuse laterally into the liposomal membrane (Figs. 4a–c) and viral contents are present at the inner liposomal surface (Fig. 5).

Because of its localization the viral matrix or M protein, a membrane protein localized at the inside of the viral membrane [6], is less likely to cause IMPs found on the concave fracture face exclusively. Instead, these IMPs more likely represent aggregates of one or both viral spike proteins. The lateral diffusion of viral spike proteins after membrane fusion is further supported by the visualization of spikes in the fractured ice-matrix surrounding the liposomes (Fig. 4a). In analogy to Sendai virus-membrane fusion [50,51], the lateral diffusion of viral spike proteins after virus-membrane fusion does not seem to be hindered by the presence of the M protein.

Acknowledgements

We thank Jan Jacobs for providing the influenza B virus suspension and Gerrit van Meer for the liposomes prepared by *n*-octyl glucoside dialysis. G.K. was supported by an EMBO long-term fellowship during his stay in Utrecht.

References

1 White, J., Kielian, M. and Helenius, A. (1983) Q. Rev. Biophys. 16, 151–195.
2 Matlin, K.S., Reggio, H., Helenius, A. and Simons, K. (1981) J. Cell Biol. 91, 601–613.
3 Mellman, I., Fuchs, R. and Helenius, A. (1986) Annu. Rev. Biochem. 55, 663–700.
4 Maeda, T., Kawasaki, K. and Ohnishi, S.I. (1981) Proc. Natl. Acad. Sci. USA 78, 4133–4137.
5 White, J., Helenius, A. and Gething, M.J. (1982) Nature 300, 658–659.
6 Compans, R.W., Klenk, H.D., Caliguiri, L.A. and Choppin, P.W. (1970) Virology 42, 880–889.
7 Rogers, G.N., Paulson, J.C., Daniels, R.S., Skehel, J.J., Wilson, I.A. and Wiley, D.C. (1983) Nature 304, 76–78.
8 Gething, M.J., White, J.M. and Waterfield, M.D. (1978) Proc. Natl. Acad. Sci. USA 75, 2737–2740.
9 Min Jou, W., Verhoeyen, M., Devos, R., Samon, E., Fang, R., Huylebroek, D., Friers, W., Threlfall, G., Carey, N. and Emtage, S. (1980) Cell 19, 683–696.
10 Wilson, I.A., Skehel, J.J. and Wiley, D.C. (1981) Nature 289, 366–373.
11 Skehel, J.J., Bayley, P.M., Brown, E.B., Martin, S.R., Waterfield, M.D., White, J.M., Wilson, I.A. and Wiley, D.C. (1982) Proc. Natl. Acad. Sci. USA 79, 968–972.
12 Wiley, D.C. and Skehel, J.J. (1987) Annu. Rev. Biochem. 56, 365–394.
13 Doms, R.W., Helenius, A. and White, J. (1985) J. Cell Biol. 260, 2973–2981.
14 White, J., Kartenbeck, J. and Helenius, A. (1982) EMBO J. 1, 217–222.
15 Heuser, J.E., Reese, T.S., Dennis, M.J., Jan, Y., Jan, L. and Evans, L. (1979) J. Cell Biol. 81, 275–300.
16 Humbel, B. and Müller, M. (1984) in Proc. 8th Eur. Congr. on Electron Microscopy (Csanady, P., Röhrlich, P. and Szabo, D., eds.), pp. 1789–1798, Budapest.
17 Cryotechniques in Biological Electron Microscopy (1987) (Steinbrecht, R.A. and Zierold, K., eds.), Springer, Berlin, Heidelberg.
18 Weibull, C., Villiger, W. and Carlemalm, E. (1984) J. Microsc. 134, 213–216.
19 Verkleij, A.J., Humbel, B., Studer, D. and Müller, M. (1985) Biochim. Biophys. Acta 812, 591–594.
20 Stegmann, T., Hoekstra, D., Scherphof, G. and Wilschut, J. (1985) Biochemistry 24, 3107–3113.
21 Van Meer, G., Davoust, J. and Simons, K. (1985) Biochemistry 24, 3593–3602.
22 Mayer, L.D., Hope, M.J. and Cullis, P.R. (1986) Biochim. Biophys. Acta 858, 161–168.
23 Böttcher, C.J.F., van Gent, C.M. and Pries, C. (1961) Anal. Chim. Acta 24, 203.
24 Struck, D.K., Hoekstra, D. and Pagano, R.E. (1981) Biochemistry 20, 4093–4099.
25 Knoll, G., Oebel, G. and Plattner, H. (1982) Protoplasma 111, 161–176.
26 Costello, M.J., Fetter, R. and Höchli, M. (1982) J. Microsc. 125, 125–136.
27 Müller, M., Marti, T. and Kriz, S. (1980) in Proc. 7th Eur. Congr. on Electron Microscopy (Brederoo, P. and De Priester, W., eds.), pp. 720–721.
28 Van Meer, G. and Simons, K. (1983) J. Cell Biol. 97, 1365–1374.
29 Haywood, A.M. and Boyer, B.P. (1981) Biochim. Biophys. Acta 646, 31–35.
30 Morgan, C. and Rose, H.M. (1968) J. Virol. 2, 925–936.
31 Bächi, T., Gerhard, W., Lindenmann, J. and Mühlethaler, K. (1969) J. Virol. 4, 769–776.
32 Knutton, S. (1976) Nature 264, 672–673.
33 Knutton, S. (1978) Micron 9, 133–154.
34 Kim, J. and Okada, Y. (1987) J. Membr. Biol. 97, 241–249.
35 Menco, B.P.M. (1987) J. Electr. Microsc. Techn. 4, 177–240.
36 Orci, L. and Perrelet, A. (1978) in Membrane Fusion (Poste, G. and Nicholson, G.L., eds.), pp. 630–651, Elsevier, North-Holland.
37 Ahkong, Q.F., Fisher, D., Tampion, W. and Lucy, J.A. (1975) Nature 253, 194–195.
38 Plattner, H. and Bachmann, L. (1982) Int. Rev. Cytol. 79, 237–304.
39 Plattner, H. (1981) Cell Biol. Int. Rep. 5, 435–459.
40 Shotton, D. (1980) Nature 283, 12–14.

41 Torri-Tarelli, F., Grohovaz, F., Fesce, R. and Ceccarelli, B. (1985) J. Cell Biol. 101, 1386–1399.
42 Knoll, G., Verkleij, A.J. and Plattner, H. (1987) in Cryotechniques in Biological Electron Microscopy (Steinbrecht, R.A. and Zierold, K., eds.), pp. 258–271, Springer, Berlin, Heidelberg.
43 Haywood, A.M. and Boyer, B.P. (1985) Proc. Natl. Acad. Sci. USA 82, 4611–4615.
44 Stegmann, T., Hoekstra, D., Scherphof, G. and Wilschut, J. (1986) J. Biol. Chem. 261, 10966–10969.
45 Krystal, M., Elliot, R.M., Benz, E.W., Young, J.F. and Palese, P. (1982) Proc. Natl. Acad. Sci. USA 79, 4800–4804.
46 Verkleij, A.J. (1984) Biochim. Biophys. Acta 779, 43–63.
47 Miller, R.G. (1980) Nature 287, 166–167.
48 Hui, S. and Stewart, T. (1981) Nature 290, 427.
49 Siegel, D.P. (1986) Biophys. J. 49, 1171–1183.
50 Bächi, T., Aquet, M. and Howe, C. (1973) J. Virol. 11, 1004–1012.
51 Henis, Y.I., Gutman, O. and Loyter, A. (1985) Exp. Cell Res. 160, 514–526.